AN ABSTRACT OF THE THESIS OF

HOSSAM H. GHALEB for the degree of Master of Science

in Physics presented on August 25, 1980

Title: Angular Correlations of Gamma Rays in the Decay of ^{193}Os

Abstract approved. Redacted for Privacy

Measurements have been made of γ-γ directional correlations of the following cascades;

(280-107) kev, (280-180) kev, (322-139) kev, (252-280) kev, (252-322) kev, (252-387) kev, (252-460) kev, (420-139) kev in ^{193}Os using Ge(Li) high resolution detectors.

From the internal conversion data and angular distribution of radiation from oriented nuclei done at Los Alamos, we calculated δ(E2/M1) the multipole mixing ratio for the above energy cascades.

The result of the measurements were:

$\delta(180) > 1.00$ $\delta(280) = 0.24 \pm 0.04$ $\delta(322) = 0.28 \pm 0.2$

$\delta(107) = 0.14 \pm 0.01$ $\delta(387) = -0.58 \pm 0.08$ $\delta(252) = 0.14 \pm 0.02$

$\delta(420) = 0.13 \pm 0.08$ $\delta(460) = -0.78 \pm 0.06$

These were compared with the equivalent decay scheme of ^{191}Ir for the energy levels with the same spins as in ^{193}Ir.

Angular Correlations of Gamma Rays in the Decay of ^{193}Os

by

Hossam H. Ghaleb

A THESIS

submitted to

Oregon State University

in partial fulfillment of
the requirements for the
degree of

Master of Science

Completed August 25, 1980

Commencement June 1981

APPROVED:

Redacted for Privacy

Professor or Physics
in charge of major

Redacted for Privacy

Chairman of Department of Physics

Redacted for Privacy

Dean of Graduate School

Date thesis presented August 25, 1980

Typed by Shanda L. Smith for Hossam H. Ghaleb.

ACKNOWLEDGEMENTS

The author wishes to express appreciation to his major professor, Dr. Kenneth Krane, for his continuous help and guidance throughout the progress of this work. To Professor Larry Schecter for his suggestions and for his encouragement which provided me with the initial momentum to do research in this field.

The author is also thankful to friends and colleagues at the Physics Department for their assistance and helpful discussions, and to the technicians in the workshop for their help.

Oregon State University Computer Center provided the grant money which was needed for computer time. Also O.S.U. Radiation Center helped with the production of the necessary radioactive samples.

Finally and above all to the Physics Department for providing me with the opportunity and the financial support throughout my stay at O.S.U.

TABLE OF CONTENTS

LIST OF FIGURES

LIST OF TABLES

ANGULAR CORRELATIONS OF GAMMA RAYS IN THE DECAY OF OS 193

I. INTRODUCTION

In this work, directional Angular Correlation measurements were used to determine the mixing ratios of the different electromagnetic transition multipoles: specifically the ratio between the E2 matrix element and the M1 matrix element.

The selection of specific isotope for this work was influenced by two factors:

1) the lack of information concerning electromagnetic properties of certain nuclei, or the existence of some conflicting results
2) the possibility of testing a nuclear model proposed by de-Shalit for certain kinds of odd-A nuclei.

Lack of precise information about ^{193}Ir hampered the effort to extract more detailed information, but nevertheless reasonably accurate δ's were found in good agreement with previous published work for ^{193}Ir.

II. THEORY OF ANGULAR CORRELATION

The probability of emission of a particle or quantum by a radioactive nucleus depends in general on the angle between the nuclear spin axis and the direction of emission. Under ordinary circumstances, the total radiation from a radioactive sample is isotropic because the nuclei are randomly oriented in space. An anisotropic radiation pattern can be observed only from an ensemble of nuclei that are not randomly oriented.

One method of arriving at such an ensemble consists of placing the radioactive sample at a very low temperature in a strong magnetic field or electric field gradient, thereby polarizing or aligning the nuclei, and then measuring the angular distribution of the emitted radiation with respect to the direction of the applied field.

Another method consists of picking out only those nuclei whose spins happen to lie in a preferred direction. This case can be realized if the nuclei decay through successive emission of two radiations R_1 and R_2. The observation of R_1 in a fixed direction k_1 selects an ensemble of nuclei that has a nonisotropic distribution of spin orientations. The succeeding radiation R_2 then shows a definite angular correlation with respect to k_1.

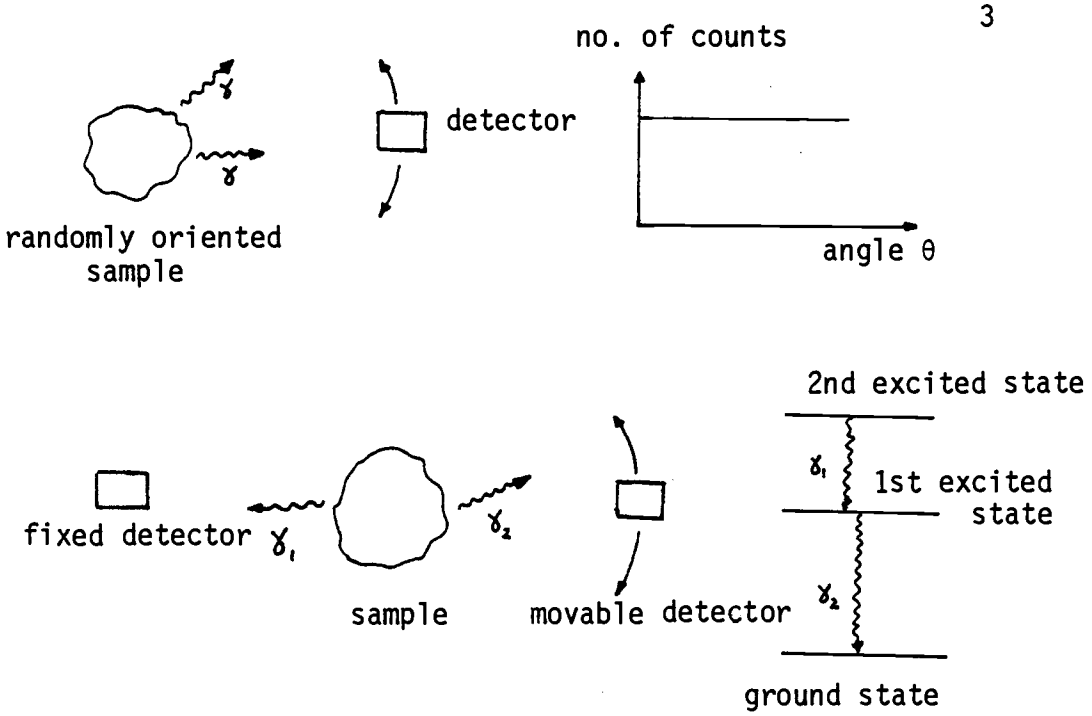

Figure 1.

The term angular correlation comprises directional correlation and polarization correlation. In directional correlation only the directions of the two radiations are observed; in polarization correlation one determines also the linear or circular polarization of one or both of the radiations.

In angular correlation work, a nucleus emits in rapid succession two γ-rays, γ_1 and γ_2. We ask for the relative probability $W(\theta)\, d\Omega$ that γ_2 is emitted into the solid angle $d\Omega$ at an angle θ with respect to k_1. The theoretical expression for the correlation function $W(\theta)$ for γ-rays has been worked out for all cases of interest (1). Experimentally one records the number of coincidences between γ_1 and γ_2 as a function of the angle θ subtended by the axes of the two counters.

Because of the finite solid angles of the counters these numbers are averages of the true correlation $W(\theta)$ over angles distributed around θ. This is true assuming axial symmetry. In case of noncentered sources, a geometrical correction must be included. Hence the coincidence counts between γ_1 and γ_2 must be properly corrected and normalized to yield $W_{exp}(\theta)$. The comparison of $W_{exp}(\theta)$ with theory finally provides the means of comparison to test validity of models which can predict the properties of the nuclear levels and the radiations.

A. Multipole Expansion of the Electromagnetic Field

When discussing directional correlation function of electromagnetic radiation the following restrictions should be kept in mind:

1) The total angular momentum and parity are assumed to have single values and to be conserved in the electromagnetic interaction.
2) The radiations are emitted in succession. The directional correlation function is defined as the probability that a nucleus decaying through a cascade $I_i \rightarrow I \rightarrow I_f$ emits the two radiations R_1 and R_2 in the directions k_1 and k_2 into solid angles $d\Omega_1$ and $d\Omega_2$.

From the theory of multipole expansion of the electromagnetic field, when the dimension of the source is small as compared

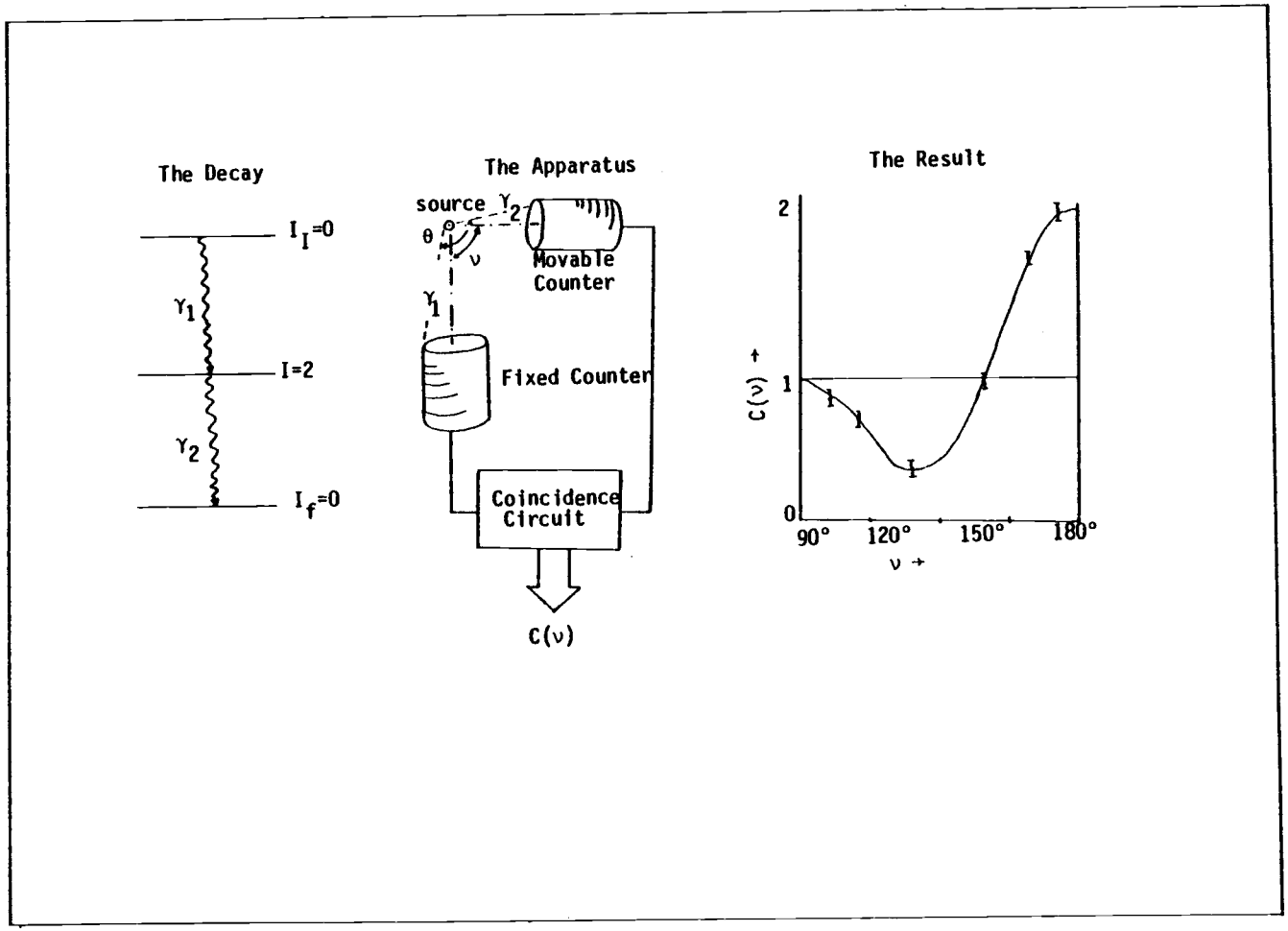

Figure 2. Example of a directional correlation measurement. (1)

to the wave length of the radiation, the field can be expanded in vector spherical harmonics (multipole expansion)

$$\vec{E}(r) = \sum_{\ell=1}^{\infty} \sum_{m=-\ell}^{\ell} a_E(\ell,m)\, \vec{E}_E(\ell,m,r) + a_m \vec{E}_m(\ell,m,r) \qquad \text{II.1.1}$$

and similarly

$$\vec{H}(r) = \frac{-i}{k\,\mu_o} \nabla \times \vec{E}(r) \qquad \text{II.1.2}$$

The functions E_E and E_m must satisfy the free wave equation:

$$\nabla^2 \vec{E} - \frac{1}{c^2} \frac{\partial^2 \vec{E}}{\partial t^2} = 0 \qquad \text{II.1.3}$$

For the same order (ℓ,m), the functions E_E and E_m correspond to solutions of different parity. That is:

$$\vec{E}_E(\ell,m,r) = (-1)^{\ell}\, \vec{E}_E(\ell,m,-r) \quad \text{electric multipole} \qquad \text{II.1.4}$$

$$\vec{E}_m(\ell,m,r) = -(-1)^{\ell}\, \vec{E}_m(\ell,m,-r) \quad \text{magnetic multipole} \qquad \text{II.1.5}$$

The power radiated by an electromagnetic source is given by the Poynting vector. Now if a pure multipole of order ℓ,m be emitted and since the coefficients for the electric and magnetic field are related we get:

$$\frac{dU(\ell,m,\theta,\phi)}{d\Omega} = \frac{1}{2\pi\omega^2 c}\, F_\ell^m(\theta,\phi)\, a(\ell,m)^2 \qquad \text{II.1.6}$$

Where $\frac{dU}{d\Omega}$ is the power emitted into the solid angle $d\Omega$ at the angle θ,ϕ and $F_\ell^m(\theta,\phi)$ is the angular distribution and is given by:

$$F_\ell^m(\theta,\phi) = \frac{1}{2}\left[1-\frac{m(m+1)}{\ell(\ell+1)}\right]|Y_\ell^{m+1}|^2 + \frac{1}{2}\left[1-\frac{m(m-1)}{\ell(\ell+1)}\right]|Y_\ell^{m-1}|^2 + \frac{m^2}{\ell(\ell+1)}|Y_\ell^m|^2 \qquad \text{II.1.7}$$

where Y_ℓ^m are the spherical harmonics.

This shows that the emitted γ-rays have an angular distribution given by the above relation.

B. Theory of γ-γ Directional Correlation in Free Nuclei

We shall start by discussing a single γ-transition of angular momentum L, between two nuclear levels i and f with spins I_i and I_f.

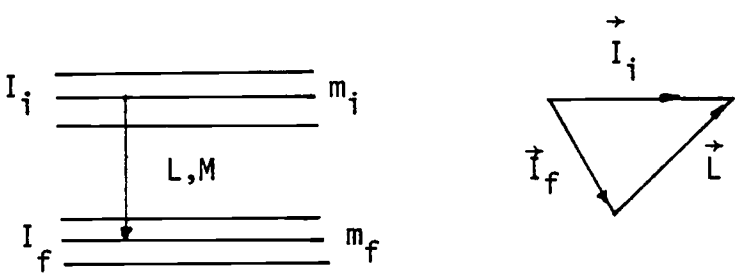

Single γ transition

Figure 3.

For conservation of angular momentum, we have $\vec{I}_i = \vec{I}_f + \vec{L}$. The projection of L on the arbitrary axis of quantization (Z-axis) shall be denoted by L_Z. The emitted γ-ray is then characterized by the angular momentum quantum number or multipolarity L,

and the magnetic quantum number M, with $L^2 = L(L+1)\hbar^2$, $L_Z = M\hbar$. The quantum numbers of the two nuclear states are I_i, m_i and I_f, m_f where $m_i = m_f + M$.

The discussion can now be extended to cascaded emission. We can obtain an oriented samples of nuclei, by applying a very strong magnetic field at low temperatures.

However, instead of attempting to orient the sample dynamically, we may select out of the sample those nuclei whose spin axis is oriented in a particular direction. This is what happens in γ-γ correlation measurement: the first γ-ray establishes, in a probability sense, the spin axis of the nucleus; then the angular distribution of the second γ-ray (obviously from the same nucleus) is measured with respect to the spin axis, which was so established by the first measurement.

For the unpurturbed directional correlation, if we know ℓ, m for the different states and using group theory calculations (2) we can arrive at the simple formula for the correlation function

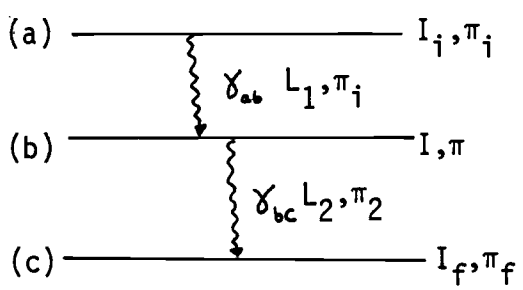

Figure 4

$$W(\theta) = \sum_{k \text{ even}} A_{kk} P_k(\cos\theta) \qquad \text{II.2.1}$$

where the angular correlation coefficients are normalized with $A_{oo} = 1$.

C. Transition Probabilities and Multipole Radiation

Consider a transition from $\frac{3}{2}^+$ s-state to $\frac{5}{2}^+$ d-state; in this case parity is not changed.

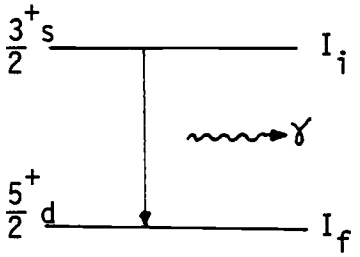

Figure 5

$I_i = \frac{3}{2} \qquad \pi_i = (-1)^{\ell} = (+)$

$I_f = \frac{5}{2} \qquad \pi_f = (-1)^{\ell} = (+)$

s state $\ell = 0$

d state $\ell = 2$

$$\Delta I_{min} = \frac{5}{2} - \frac{3}{2} = 1$$

$$\Delta I_{max} = \frac{5}{2} + \frac{3}{2} = 4$$

The parity of the emitted γ-ray is then given by:

$$\pi = \pi_i \, \pi_f = (+)$$

and the angular momentum L of the γ-ray can have any integer value between 1 and 4. By using equations II.1.4, II.1.5, the possible electric and magnetic multipole radiations are given in the following table.

L	1	2	3	4
$E_L(-1)^L$	-	+	-	+
M_L-$(-1)^L$	+	-	+	-

Table 1.

Since the outgoing γ-ray has a positive parity, then the possible transitions are M1, E2, M3, E4.

The transition probability for an electric or magnetic multipole of a single particle transition is given by Weisskopf's formula which in general can be written in the following form:

$$\Gamma_{\gamma W}(EL) = N(E,L)\, A^{2L/3}\, E_\gamma^{2L+1}\, e\, v \qquad \text{II.3.1}$$

$$\Gamma_{\gamma W}(ML) = N(M,L)\, A^{\frac{2(L-1)}{3}}\, E_\gamma^{2L+1}\, e\, v \qquad \text{II.3.2}$$

where E_γ is in Mev units and the constants N(E,L), N(M,L) are given by the following table (3):

L	N(E,L)	N(M,L)
1	6.8×10^{-2}	2.1×10^{-2}
2	4.9×10^{-8}	1.5×10^{-8}
3	2.3×10^{-14}	6.8×10^{-15}
4	6.8×10^{-21}	2.1×10^{-21}
5	1.6×10^{-27}	4.9×10^{-28}

Table 2. (3)

From the previous example one can show that E2 + M1 in a transition which do not change parity, is a dominant transition.

The coefficients A_{kk} in the expansion of the angular correlation function $W(\theta)$ are given by:

$$A_{kk} = B_k(\gamma_1) \cdot A_k\,(\gamma_2) \qquad \text{II.3.3}$$

where γ_1, γ_2 are the two gamma rays in cascade. B_k and A_k are then given from nuclear orientation considerations by

$$A_k(\gamma_2) = \frac{F_k(LLI_fI_i) + 2\delta_2 F_k(LL'I_fI_i) + \delta_2^2 F_k(L'L'I_fI_i)}{1 + \delta_2^2} \qquad \text{II.3.4}$$

where L is the order of multipole and L' = L + 1. I_f, I_i are the final and initial spins of the levels under investigation.

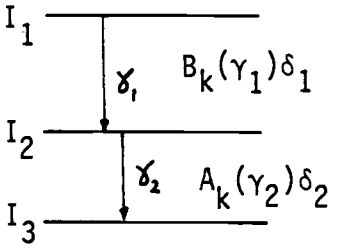

Figure 6.

Also

$$B_k(\gamma_1) = \frac{F_k(LLI_iI_f) - 2\delta_1 F_k(LL'I_iI_f) + \delta_1^2 F_k(L'L'I_iI_f)}{1 + \delta_1^2} \qquad \text{II.3.5}$$

and the mixing ratio δ is defined as the ratio of two multipole components $\pi L, \pi' L'$ for electric or magnetic multipole respectively and is given by:

$$\delta = \frac{\langle I_f \,||\, \pi L \,||\, I_i \rangle}{\langle I_f \,||\, \pi' L' \,||\, I_i \rangle} \qquad \text{II.3.6}$$

III. EXPERIMENT AND EQUIPMENT

A typical experimental set-up for gamma rays is shown in Figure 7. The gamma rays γ_1 and γ_2 are counted in counters 1, 2. The output of these counters are divided into a "slow" channel and coincidence (time to pulse amplitude converter) channel. The slow channel uses linear amplifiers to preserve the pulse height and determine the energies of γ_1 and γ_2. The output of the TAC and the output of the single channel analyzers are fed into a coincidence circuit. An output signal results only if the gamma rays possess proper energies and if the pulses are simultaneous within the resolving time. These output signals $C(\theta)$, measured as a function of the angle θ and properly correlated, yield the directional correlation function $W(\theta)$.

A. Detectors and Preamplifiers

The detectors in this experiment are lithium drifted germanium semiconductor junctions, "Ge(Li) detectors." The advantage of these detectors over scintillation type counters is the superior energy resolution obtained, which makes the investigation of more complicated decay schemes easier.

One of the main disadvantages of a Ge(Li) detector is that the low atomic number of germanium gives a small probability for the radiation to interact with the detector. The efficiency

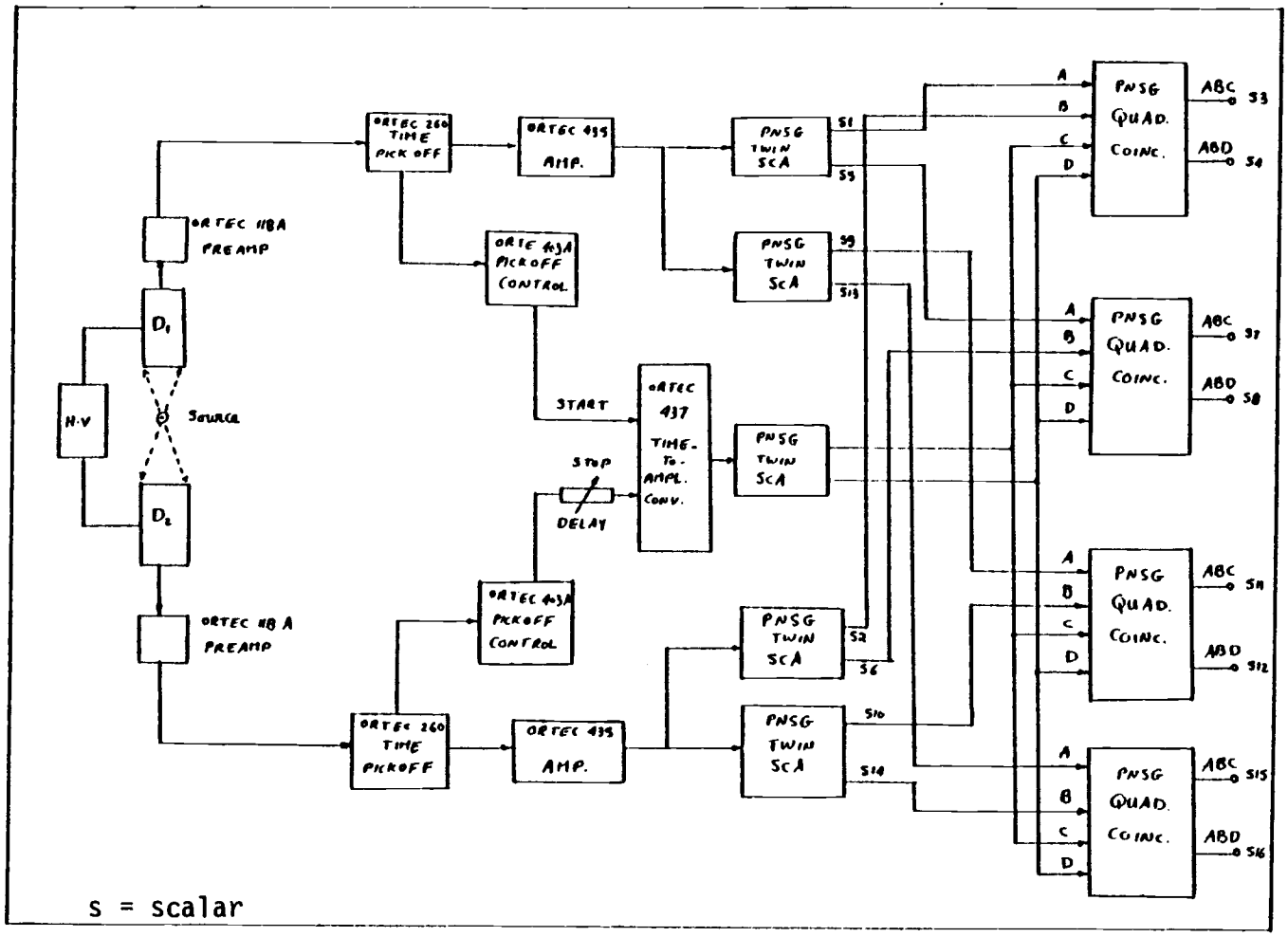

Figure 7. Block diagram of electronics.

is lower than that of a NaI detector by a factor of 10, so that it can be used only with strong gamma sources.

The resolution of lithium-drifted germanium detectors is ten to twenty times better than has been obtainable with sodium iodide scintillation crystals. Their pulse rise-times are a few tens of nanoseconds, about ten times as fast as the sodium iodide scintillation (~250 nsec), so that germanium detectors are more useful in coincidence experiments.

Optimum performance of Ge(Li) detectors is achieved by placing the detector in thermal contact with a tank of liquid nitrogen.

The efficiency of a Ge(Li) detector falls sharply as the energy of the incident radiation increases, and the probability for detecting high energy gamma rays becomes small.

A gamma-ray spectrum obtained with a Ge(Li) detector is shown in figure 11.

B. Pulse Height Analysis

The height of the output pulse from a linear amplifier connected to a detector is proportional to the energy dissipated by the nuclear radiation within the detector, and so the energy distribution curves (nuclear spectra) may be obtained by measuring the amplitudes of the output pulses.

The process of pulse height analysis can be divided into two stages - amplification and shaping of pulses, and selection

of desired amplitude to represent a given energy loss in the detector.

When selecting an amplifier three characteristics have to be considered carefully; linearity, stability, and minimum introduction of noise. These were achieved by using an active filter amplifier. Selection of an energy region was accomplished by using single-channel analyzers (SCA).

C. Timing and Coincidence Circuits

A coincidence or logic unit generates an exactly timed output signal whenever the time overlap of input signals satisfies a preselected coincidence requirement.

The selection of the timing pulses which occur simultaneously (or within a certain resolving time) in the two detectors is performed in the fast coincidence circuit. This was achieved by using a time to amplitude converter (TAC), which gives an output signal whose amplitude is directly proportional to the time difference between the two input signals.

The flat background shown in Figure 8 is a result of the accidental coincidences (chance); these are events which do not come from the same nucleus.

A twin single-channel analyzer is used to provide the "slow" coincidence circuit with the outputs corresponding to regions A and B in the spectrum as shown in Figure 8. These signals

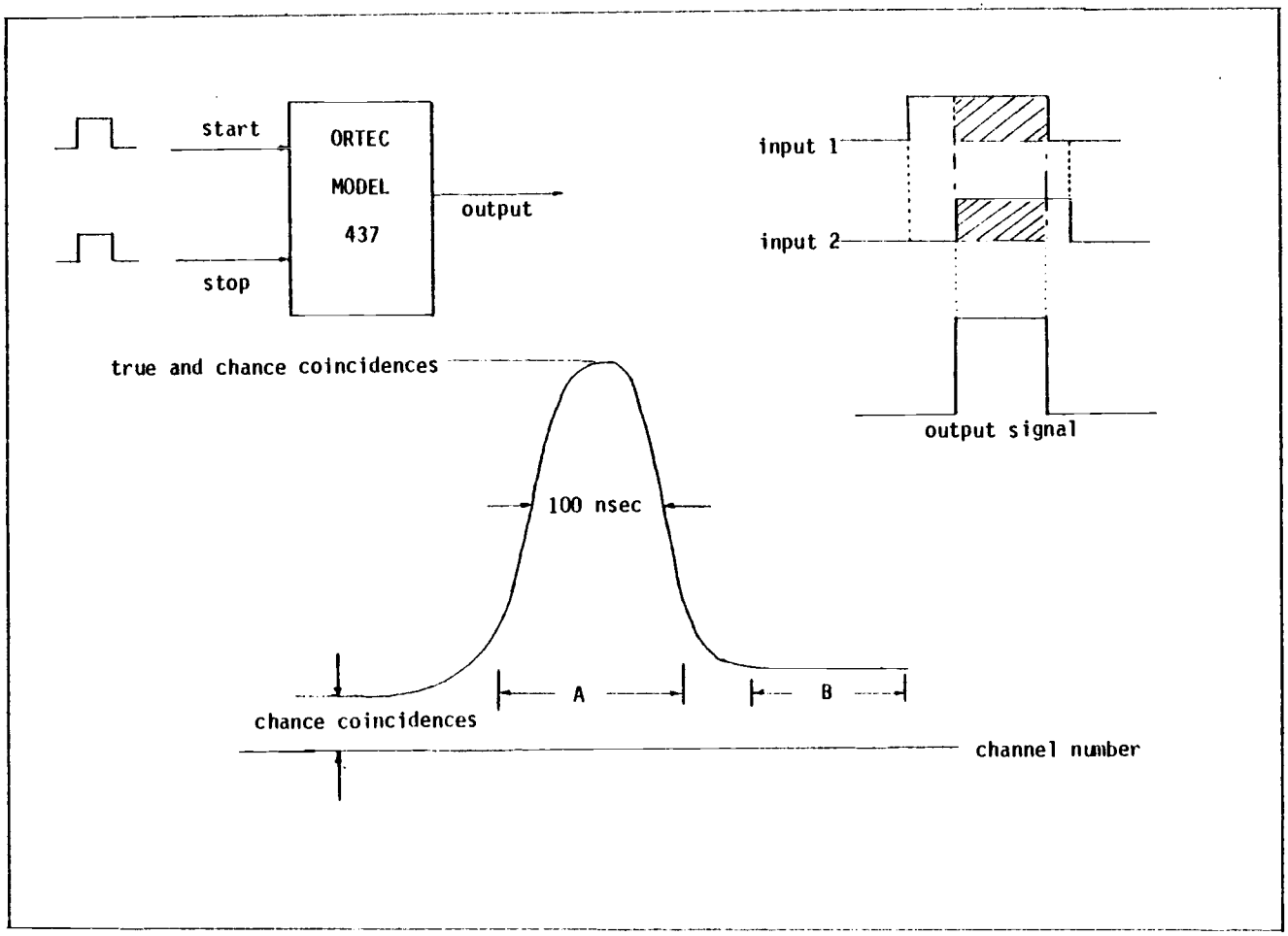
start
stop
ORTEC
MODEL
437
output
input 1
input 2
output signal
true and chance coincidences
100 nsec
A
B
chance coincidences
channel number

Figure 8.

are then fed to a coincidence circuit in which the outputs represent chance events and true plus chance events (Figure 9).

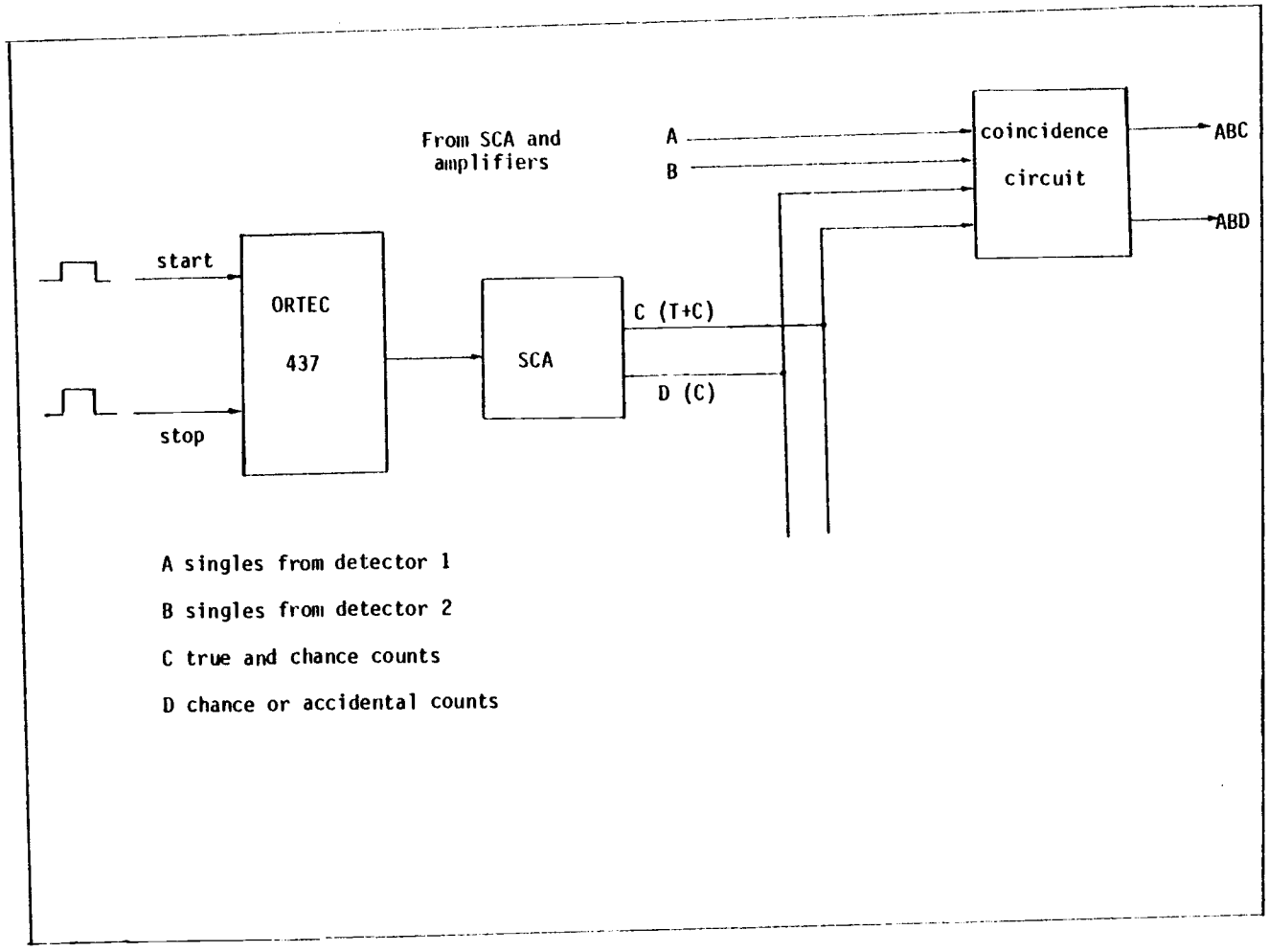
From SCA and
amplifiers
A
B
coincidence
circuit
ABC
ABD
start
stop
ORTEC
437
SCA
C (T+C)
D (C)
A singles from detector 1
B singles from detector 2
C true and chance counts
D chance or accidental counts

Figure 9.

IV. SOURCE PREPARATION AND CALIBRATION

The radioactive source employed in this experiment was ^{193}Os. It was obtained by irradiating ^{192}Os powder in the nuclear reactor at the Radiation Center of Oregon State University.

^{192}Os metal powder (160 mg) was placed in the nuclear reactor for 1 hour at 1 Megawatt continuous (dc) power to produce ^{193}Os through the ^{192}Os(n,γ)^{193}Os nuclear reaction. (A small amount of radioactive ^{191}Os is also produced due to the natural abundance of ^{190}Os in the sample. This gives rise to a 129 kev-γ-ray which is identified in the spectrum shown in Figure 11.) The sample is placed in a special radioactive isotope production port where thermal neutrons are utilized in the reaction.

The source was mounted on an adjustable platform which could be moved by screw adjustments in the plane of the correlation table along two perpendicular axes in the 90° direction and 180° direction. This arrangement was used to center the source relative to the arc traversed by the movable detector. (0° is defined by the source-fixed detector line).

The criterion for source centering was set at 1 percent maximum deviation in the singles counting rate of the movable detector at 90°, 180°, 270°. Vertical centering was accomplished by varying the height at which the rod was held in the support

platform, so that the geometrical center of the source was at the same height as the cylinder axis of the detector cryostat.

Alignment and finite resolution detector effects were determined by using a ^{22}Na positron source. The two 511 kev photons produced when positrons annihilate are emitted in opposite directions; thus a coincidence experiment between the two photons using a point source and point detectors would yield a delta-function peaked at 180°. However, a finite angular resolution of real detectors causes the distribution to spread, with the center of the distribution remaining at 180°. The source was centered relative to the movable detector, using the singles counting rates as described before. A coincidence experiment was then performed between 511 kev photons and the coincidence counting rates were measured at two symmetric positions on either side of 180°, normally 165°, 195°. The fixed detector was then moved laterally until these coincidence counting rates were equal to within statistical counting errors.

Since the efficiency of a Ge(Li) detector falls off rapidly with increasing energy above 200 kev, low energy X-rays have a relatively great probability of being detected and their high counting rates can cause large dead times in the electronics, as well as adversely affect the true to chance ratio. To eliminate this problem absorbers were placed on the front of the detector cryostats, which served to stop the X-rays without seriously affecting the gamma-rays under investigation. Normally copper and lead metal foils were used.

A. Solid Angle Correction Factors for Coaxial Ge(Li) Detectors

Owing to the finite solid angle subtended by a radiation detector, the observed angular distribution will differ somewhat from the ideal distribution expected for point detectors. The proper interpretation of precision angular distribution measurements thus depends on the accurate knowledge of this difference, in order to correct the observed distribution for effects due to the finite size of the radiation detectors.

Since the angular correlation curve is theoretically given as:

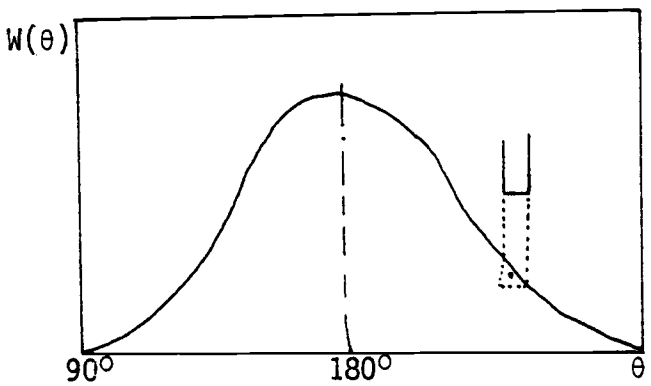

Figure 10

due to the finite size of the detectors, the measured values of the angular correlation coefficients A'_{kk} will always be less than the theoretical value A_{kk}.

The measured angular correlation function in this case is:

$$W(\theta) = A'_{oo} + A'_{22} P_2(\cos\theta) + A'_{44} P_4(\cos\theta) + \ldots \quad \text{IV.1.1}$$

and the actual value for A_{kk} is then:

$$A_{kk} = \frac{A'_{kk}}{Q_{kk}} \qquad \text{IV.1.2}$$

where Q_{kk} can be calculated from the following relationship:

$$Q_{kk} = Q_{kk}(511 \text{ kev}) \frac{Q_k(E\gamma_1)}{Q_k(511 \text{ kev})} \frac{Q_k(E\gamma_2)}{Q_k(511 \text{ kev})} \qquad \text{IV.1.3}$$

where both $Q_{kk}(511 \text{ kev})$ and $Q_k(511 \text{ kev})$ were determined from the geometrical correction experiment using the ^{22}Na source.

In general, the Q_k correct for all geometric effects on the observed distribution function, including finite source size as well as finite detector size.

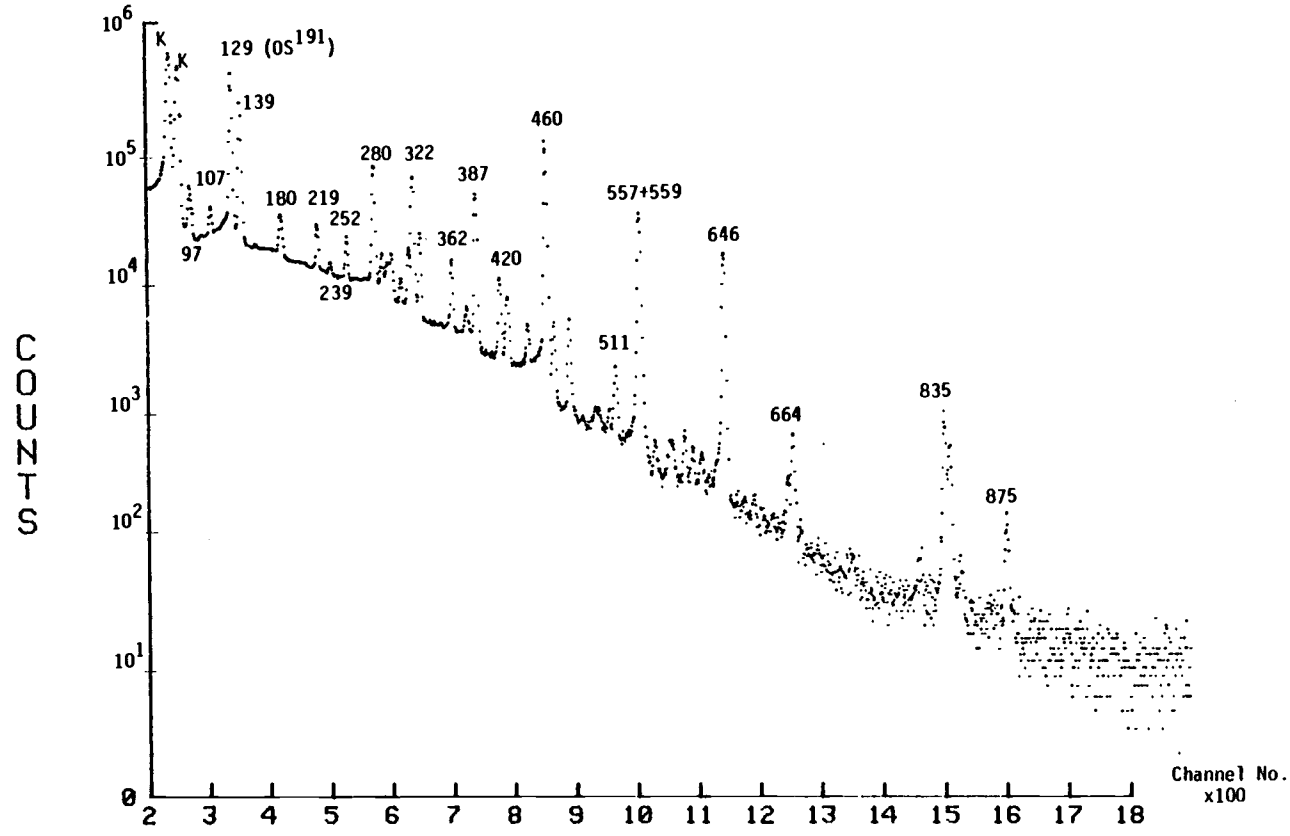

Figure 11. ^{193}Os spectrum

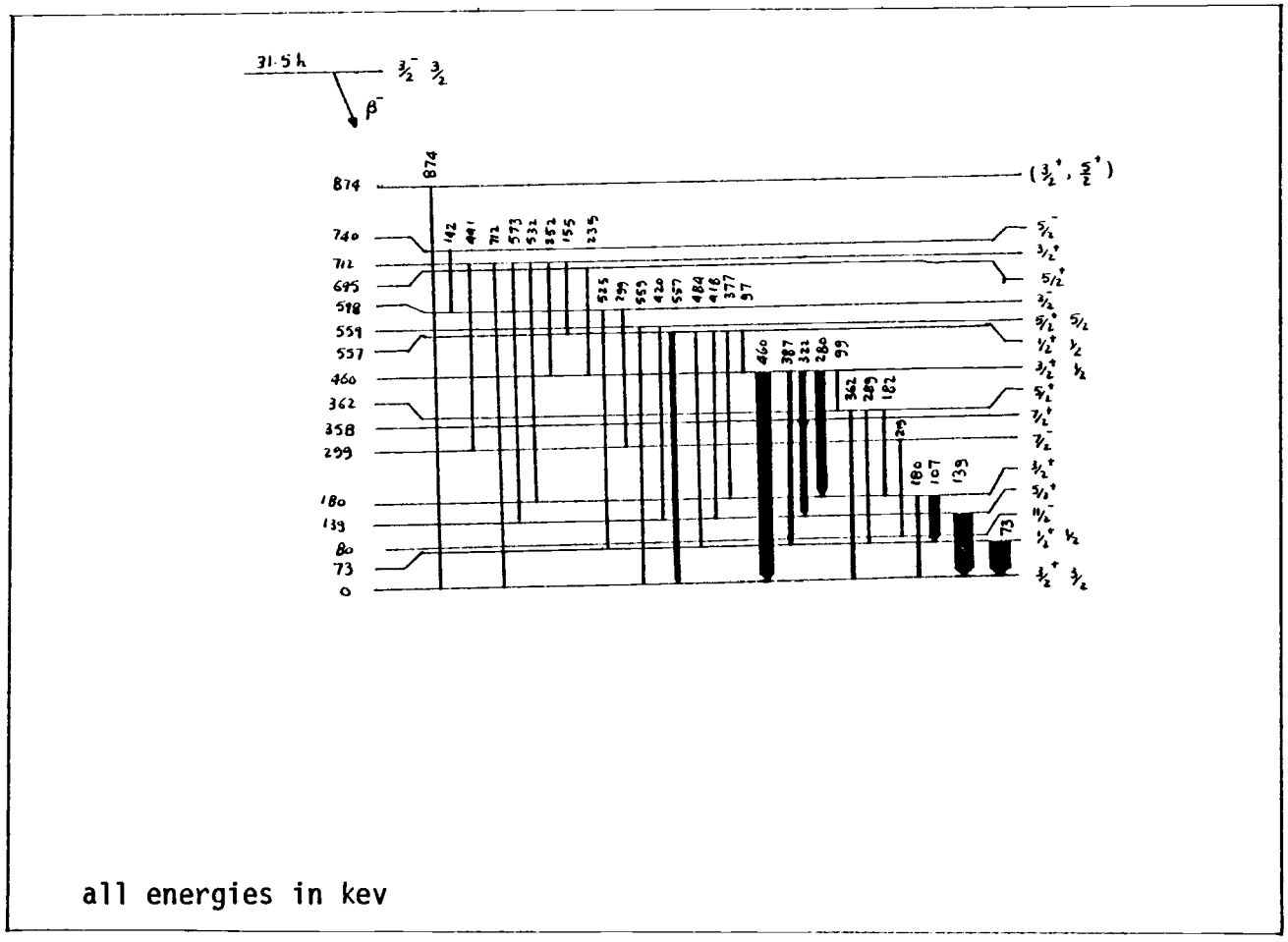

Figure 12. Decay scheme of ^{193}Os

V. ^{193}Os DECAY SCHEME

Figure 11 shows the gamma spectrum of the decay of ^{193}Os as it would be found on the multichannel analyzer. Also the decay scheme shows transition energies and relative intensities of radiation (dark lines more intense). Previous work which has been done on this decay scheme include the Los Alamos nuclear orientation experiment, the conversion electron experiments, gamma-ray spectroscopy, and previous gamma-gamma angular correlation experiments. The decay of ^{193}Os to levels of ^{193}Ir is shown in Figure 12, taken from K.S. Krane and W.A. Steyert (2.)

A. Internal Conversion Experiments

As will be seen in the discussion of results, it was necessary to start with a well known value of δ. The 139 kev transition was used for this purpose with a value of $\delta(139) = -0.32 \pm 0.02$. This magnitude is an average of previous published data of internal conversion experiments (5), (6), (7), (8), (9). The sign was also determined previously (2).

The electromagnetic transitions in the nucleus are of two main types:

(1) Emission of gamma ray of energy E_γ, and angular momentum L is referred to as pure multipole emission.

(2) Internal conversion of an orbital electron, with energy in the continuum - $E_\gamma - E_B$ and angular momentum

$I_f = L + I_i$, where I_f, I_i are the final and initial nuclear angular momentum and E_B is the binding energy of the electron.

The two processes (1), (2) are competitive and the branching ratio of process (2) to (1) is the internal coefficient α. α may be any positive number. The internal conversion process is fully analogous to the Auger effect. The only difference is that instead of two electrons making a transition, one electron and the nucleus are involved.

In general the coefficients increase strongly with Z. For the K-shell α varies like Z^n where n depends slightly on E and L but is approximately 3. The origin of this dependence is simply the density of K-shell electrons near the nucleus. Table 3 shows previously measured δ using this technique.

B. Nuclear Orientation Studies

Observation of the angular distribution of radiation emitted by nuclei polarized at low temperatures is a convenient means to study nuclear properties such as spins, moments, and radiation multipolarities.

In nuclear orientation experiments, nuclei are cooled to a very low temperature and subjected to a high magnetic field, radiation from the aligned nuclei can then be studied.

The expression for angular distribution of gamma radiation emitted by an oriented nuclear state is given by:

Table 3. Summary of Results

Transition Energy (kev)	Multipolarity	E2 %			$\|\delta\|$		
		Lower Bound	Calc. (given)	Upper Bound	Lower Value	Calc. Value	Upper Value
107 kev	M1 + E2	2	3	4	0.14	0.18	0.20
		0	6	16	0	0.25	0.44
		2	3	4	0.14	0.18	0.20
		-	-	-	0.12	-	0.16
		1.8	2.2	2.6	0.14	0.15	0.16
		1.3	1.7	2.1	0.11	0.13	0.15
139 kev	M1 + E2	11	13	16	0.35	0.39	0.44
		1	9	20	0.10	0.31	0.50
		7	8	9	0.27	0.29	0.31
		-	-	-	0.32	-	0.34
		10	11	12	0.33	0.35	0.37
		-	-	-			
		8.3	9.1	9.9	0.30	0.32	0.33
					av.	0.32±.02	
180 kev	M1 + E2	-	-	-	-	-	-
		12	17	22	0.37	0.45	0.53
		-	-	-	1.02	-	1.13
		23	35	47	0.55	0.73	0.94
		-	-	-		1.08±.06	
		12	20	28	0.37	0.50	0.62

Accuracy of δ is determined by upper and lower bounds of E2%.

Table 3 continued

252 kev	M1 + E2	-	-	-	-	-	-
		0	0	50	0	0	1.00
		0	12	24	0	0.13	0.56
		-	-	-	0.56	-	0.97
		-	4±4-17%	-	-	0.20	-
		-	24	-	-	0.56	-
280 kev	M1 + E2	20	30	40	0.50	0.65	0.82
			2		0.03	0.14	0.18
		9	12	15	0.31	0.37	0.42
		-	-	-	0.59	-	0.87
		0	10	20	0	0.33	0.50
		-	10	0	-	0.33	-
322 kev	M1 + E2	20	30	40	0.50	0.65	0.82
		-	2.3	-	0.10	0.15	0.44
		0	5	10	0	0.23	0.33
		-	-	-	0	0	0.71
		7	20	33	0.27	0.50	0.70
		-	8	-	-	0.29	-
460 kev	M1 + E2	10	20	30	0.33	0.50	0.65
		-	25	-	0.10	0.58	0.96
		10	17	24	9.33	0.45	0.56
		-	-	-	0.76	-	0.96
		11	24	37	0.35	0.56	0.71
		10	17	24	0.33	0.45	0.56

$$W(\theta) = \sum_k Q_k B_k U_k A_k P_k(\cos\Theta) \qquad V.2.1$$

where the B_k specify the orientation of the initial level, U_k correct for the effect of unobserved intermediate radiations, and the A_k describe the properties of the observed gamma rays. Q_k are the solid-angle correction factors, and the P_k are the ordinary Legendre Polynomials.

Present work is needed for analysis of the Los Alamos data (4). The nuclear alignment data measure only U_2A_2 (or $B_2U_2A_2$), and to get the gamma ray mixing ratios, we need to use a gamma ray of known (or measured) A_2 to find B_2U_2, which can then be employed to analyze the rest of the gamma rays.

The following tables show $B_2U_2A_2$ and δ for different energy transitions from the Los Alamos nuclear orientation data.

TABLE 4. Angular distribution anisotropies from the decay of oriented ^{193}Os (2).

γ ray (kev)	$B_2U_2A_2$[a] (units of 10^{-3})
107	38(10)
139	197(1)
180	70(5)
252	-117(2)
280	-68(1)
322	40(1)
387	111(1)
418+420	-95(3)
460	47(1)

[a]Figures in parentheses are uncertainties in last digit or digits.

TABLE 5. E2/M1 multipole mixing ratios of ^{193}Ir γ rays (2).

γ-ray energy (kev)	δ(E2/M1)
107	+0.141±0.010
139	-0.34 ±0.01
180	$-(0.67^{+0.24}_{-0.14})$
252	$-0.07 \leq \delta \leq +0.07$
280	+0.60 ± 0.033
322	+0.157± 0.025
387	-0.21 ± 0.07
420	+0.27 ± 0.01
460	-0.54 ± 0.04

VI. DATA ANALYSIS

The raw data accumulated through the experiment using the ^{193}Os source were analyzed using computer programs of Dr. K. Krane. The Cyber 73 computer on campus and the facilities of the Computer Center were used to analyze the data. Analyzing the data to calculate the angular correlation coefficients A_{kk} and the mixing ratios δ was done in three steps: 1) reduction of the raw data to counting rates at each angle; 2) computing the coefficients A'_{kk} from counting rates; and 3) the determination of the geometric correction factors Q_{kk} to calculate the exact value of A_{kk}.

The number of individual runs amounted to 30 runs. Each run measured 4 energy cascades at different angles 90°, 120°, 150°, 180°, 210°, 240°, 270°; the raw data were then condensed to one net counting rate per angle. Several operations were performed on the data to compensate for possible errors.

1. Compensation for the radioactive decay ($t_{\frac{1}{2}}$ = 31.6 hrs) of the source during the course of the measurement. This was done by using a $\frac{1}{2}$-life correction in the analysis program, or by using a ratio of the single counts to indicate the decaying of the source.

2. Elimination of data points with large deviations. This was accomplished by setting a criterion of 1 percent root-mean-square deviation from average. To prevent the introduction of

systematic errors by rejecting large numbers of data points, it was decided to set an upper limit on the number of runs which could be rejected at any given angle.

After the data pass the statistical test, the coincidence data were normalized and then once the counting rates and errors had been determined it was necessary to fit the measured counting rates to a relationship of the form:

$$W(\theta) = \sum_{k \text{ even}} A'_{kk} P_k(\cos\theta)$$

where the angular correlation coefficients are normalized with $A'_{oo} = 1$.

Then the weighted average of A'_{22}, A'_{44}, $A'_{22}(A'_{44}=0)$ for all the runs was computed.

Using internal conversion data for 139 kev transition and the nuclear orientation data from Los Alamos we were able to calculate δ for the different energy levels of ^{193}Ir. The following table shows the weighted averages for A_{22}, A_{44}

Table 6.

Energy Levels kev	A_{22}	A_{44}
280-107	-0.073±-0.021	0.011±-0.016
280-180	-0.156±-0.021	-0.069±-0.031
322-139	0.726±-0.017	-0.038±-0.031
420-139	-0.317±-0.044	-0.114±-0.065
252-322	-0.193±-0.034	0.025±-0.050
252-387	0.103±-0.042	-0.047±-0.063
252-280	-0.095±-0.035	0.079±-0.054
252-460	-0.196±-0.026	-0.035±-0.041

VII. RESULTS

Starting with $\delta(139\text{ kev}) = -0.32\pm0.02$ for 139 kev transition taken from internal conversion data given by Table 3 and knowing that:

$$A_{22} = B_2(\gamma_1) \cdot A_2(\gamma_2) \qquad \text{VII.1}$$

we were able to calculate A_2, B_2, δ for the different transitions. The measured cascades are individually analyzed below.

322-139 kev: Knowing the value of $\delta(139)$ from ICC $(\frac{5^+}{2} \rightarrow \frac{3^+}{2})$, from tables of F coefficients (10) we were able to calculate $\delta(322)$, the values of A_2 and B_2 were:

$A_2 = 0.87 \pm 0.02$ (from II.3.4 with $\delta(\gamma_2 = 139\text{ kev})$)

$B_2 = 0.83 \pm 0.03$ (from VII.1 and table 6)

The multipole mixing ratio of 322 kev transition is deduced to be:

$\delta(322) = 0.28 \pm 0.02$ (from II.3.5)

280-180 kev: To calculate $\delta(280)$ we used data from the nuclear orientation experiment (4) done at Los Alamos.

Since the 322 kev transition and 280 kev start from the same level which is produced by a β^- decay, then:

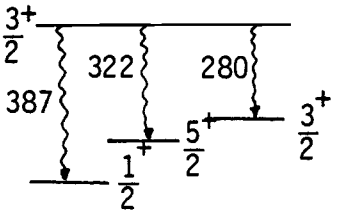

Figure 13

$$\frac{B_2U_2A_2(280)}{B_2U_2A_2(322)} = \frac{A_2(280)}{A_2(322)} = \frac{-0.068 \pm .001}{0.040 \pm .001} = -1.70 \pm 0.05$$

With our determined $\delta(322)$ and II.3.4. we found

$$A_2(322) = 0.43 \pm 0.02$$

It follows that $A_2(280) - 0.07 \pm 0.04$ and then $\delta(280) = 0.24 \pm 0.04$.

To calculate $\delta(180)$, using $A_{22}(280\text{-}180)$ from table 6 as -0.156 ± 0.021, $B_2(280)$ was calculated and hence $A_2(180)$. It follows that $\delta(180) > 1.00$.

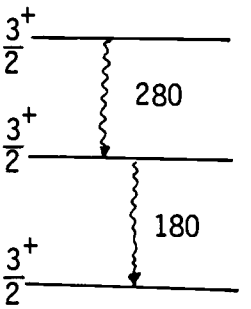

Figure 14

252-460 kev: To calculate $\delta(460)$ we started from nuclear orientation data and the ratio of $A_2(460)$ to $A_2(322)$ was then found to be:

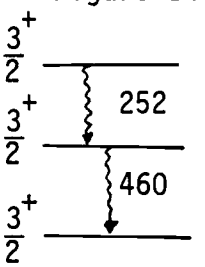

Figure 15

$$\frac{B_2U_2A_2(460)}{B_2U_2A_2(322)} = \frac{A_2(460)}{A_2(322)} = \frac{0.047 \pm .001}{0.040 \pm .001} = 1.18 \pm 0.04$$

it followed that $A_2(460) = 0.50 \pm 0.03$

$\delta(460)$ was then found to be

$$\delta(460) = -0.78 \pm 0.06$$

with $A_{22}(252\text{-}460) = -0.146 \pm 0.026$

a value for $\delta(252)$ was calculated and found to be:

$$\delta(252) = 0.07 \pm 0.03$$

252-280 kev: Since $A_{22}(252\text{-}280) = .095 \pm .035$ $A_2(280)$ was calculated $A_2(280) = -0.72 \pm 0.04$ and $B_2(252)$ can then be calculated

$B_2(252) = 0.13 \pm 0.05$

it follows that $\delta(252) = 0.35 \pm 0.04$

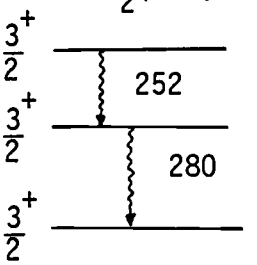

Figure 16

252-322 kev: From experimental data $A'_{22}(252\text{-}322)$ and $Q_{22}(252\text{-}322)$ which resulted in a value for $A_{22}(252\text{-}322) = -0.193 \pm 0.034$ since $A_2(322)$ known from before, $B_2(252)$ was found to be $B_2(252) = -0.45 \pm 9.08$ and hence a value for $\delta(252)$ can be calculated

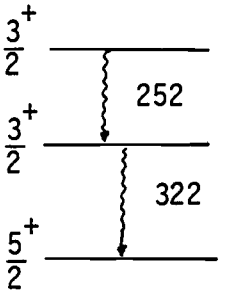

Figure 17

$\delta(252) = -0.34 \pm 0.06$

252-387 kev: To calculate $\delta(387)$ we started by finding the ratio of $A_2(280)$ to $A_2(387)$

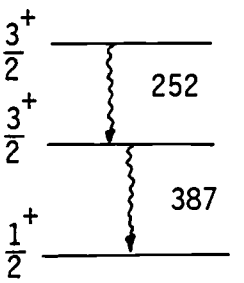

Figure 18

$$\frac{A_2(280)}{A_2(387)} = \frac{-0.068 \pm .001}{0.111 \pm .001} = -0.61 \pm 0.01$$

since $A_2(280)$ known from previous results a value for $A_2(387)$ was calculated

$A_2(387) = +1.18 \pm 0.07$

and hence $\delta(387) = -0.58 \pm 0.80$

since $A_{22}(252\text{-}387) = 0.103 \pm 0.042$, we calculated $B_2(252)$ and the result was $B_2(252) = 0.08 \pm 0.04$, then $\delta(252) = 0.20 \pm 0.02$

An average value for $\delta(252)$ was calculated which resulted in $\delta(252) = 0.15 \pm 0.02$

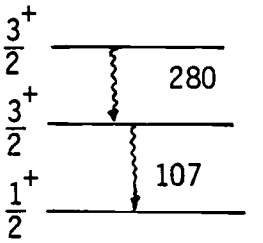

Figure 19

280-107 kev: Here we started with a known value for $\delta(107) = +0.141 \pm 0.01$ since $A_{22}(280\text{-}107) = B_2(280) \cdot A_2(107)$ $B_2(280)$ was calculated from nuclear orientation F. coefficients

$$B_2(280) = -0.03 \pm 0.06$$

and $A_2(107) = 0.24 \pm 0.02$

a value for $A_{22}(280\text{-}107)$ was calculated and found to be:

$$A_{22}(280\text{-}107) = -0.006 \pm 0.014$$

which compared to $A_{22}(280\text{-}107)$ calculated from measured value $A'_{22}(280\text{-}107)$ gave $A_{22}(280\text{-}107) = -0.073 \pm 0.011$

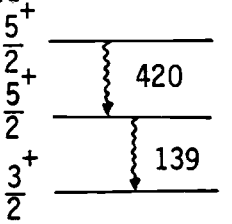

Figure 20

420-139 kev: The 429 kev level is actually composed of two closely spaced levels; 418 kev level of pure E2 ($\delta=\infty$), 420 kev level with a mixing ratio (i.e. E2+M1 exist). The angular correlation coefficient in this case is:

$$A_{22}(420\text{-}139) = B'_2(420) \cdot A_2(139)$$

where $B'_2(420) = f\, B_2(418 + (1\text{-}f)\, B_2(420)$

where f is the ratio of intensities I(418) to I(420).

Since $A'_{22}(420\text{-}139) = -0.291 \pm 0.041$

and $A_2(139) = 0.87 \pm 0.02$ we were able to calculate $A_{22}(420\text{-}139)$ which resulted in $A_{22}(420\text{-}139) = -0.317 \pm 0.044$. From (4) the ratio f is calculated using $I(418) = 0.5 \pm 0.1$, $I(420) = 1.6 \pm 0.3$

i.e., $f = 0.31 \pm 0.09$

from which $B'(420) = -0.36 \pm 0.05$ and hence $B_2(420) = 0.29 \pm 0.09$, it follows that $\delta(420) = 0.13 \pm 0.08$.

The following table compares the values of the mixing ratio δ(E2/M1) in identical transitions of ^{191}Ir and ^{193}Ir

Table 7. (15)

Level	^{191}Ir		^{193}Ir	
	E_γ(kev)	δ	E_γ(kev)	δ
$(\frac{5}{2})_1 - (\frac{3}{2})_1$	129	-0.403±0.004	139	-0.32 ± 0.02
$(\frac{3}{2})_2 - (\frac{3}{2})_1$	179	-0.75 ± 0.03	180	> 1
$(\frac{3}{2})_2 - (\frac{5}{2})_1$	97	+0.141± 0.009	107	+0.14 ± 0.01
$(\frac{3}{2})_3 - (\frac{3}{2})_1$	539	-0.68 ± 0.02	460	-0.78 ± 0.06
$(\frac{3}{2})_3 - (\frac{1}{2})$	457	-0.32 ± 0.04	387	-0.58 ± 0.08
$(\frac{3}{2})_3 - (\frac{3}{2})_2$	409	+0.184 ± 0.006	322	+0.28 = 0.02
$(\frac{3}{2})_3 - (\frac{5}{2})_1$	360	+0.023 ± 0.009	280	+0.24 ± 0.04
			420	+0.13 ± 0.08
			252	+0.15 ± 0.02

VII. CONCLUSION

In the present work several multipole mixing ratios δ(E2/M1) have been determined for gamma-ray transitions in ^{193}Ir. In order that these results can be used for calculations of the nuclear structure of ^{193}Ir excited states, additional data on transition probabilities and life times are required.

Results were compared with the equivalent transitions in the decay scheme of ^{191}Ir. One can also compare our findings with previous published data of the conversion electron experiments. Since the nuclear structure of ^{191}Ir and ^{193}Ir differs only by two neutrons, the values of δ for both isotopes were expected to be similar. Most noticeable disagreement with previous results occurred at δ(180) which showed a value > 1.00, this may be due to unresolved gamma-rays which we did not account for, or that the previous result is not accurate.

More work using high resolution detectors has to be done to determine δ(180) and δ(280), also to study cascades (280-180 kev) and (280-107 kev).

REFERENCES

1) Sigbahn, Alpha-Beta and Gamma ray Spectroscopy (North Holland Publishing Co. 1965) pp. 997-1001.

2) Adrian Melissionos, Experiments in Modern Physics (Academic Press 1966) pp. 424-429.

3) M.A. Preston, Physics of the Nucleus (Addison-Wesley Publishing Co. 1963) pp. 336.

4) K.S. Krane, W.A. Steyert, Physical Review C 7, 1555 (1973).

5) R. Avida, J. Burde, A. Molchadzki and Z. Berdnt, Nuc. Phy. A 114, 365-376 (1968).

6) R.H. Price, M.W. Johns, N.H. Ahmed and E.E. Habib Canadian Jor. of Phy., vol. 47, (1969).

7) H.J. Hennecke and J.C. Manthurthil, Phy. Rev., vol. 182, 4, (1969).

8) R. Avida, M.B. Gouldberg, G. Goldring and A. Springzak, Nuc. Phy. A 135, 678-688 (1969).

9) V. Berg and S.G. Mamskag, Nuc. Phy. A 143, 177-210, (1970).

10) K.S. Krane, LA-4677, UC-34, (1971).

11) Aai Hung Chang, Basic Nuclear Electronics (Wiley Interscience 1969).

12) G.D. Greenly, D.C. Northrop Semiconductor Counters for Nuclear Radiations (Hazell Watson & Viney Ltd. 1963).

13) K.S. Krane, Ph.D. thesis, Purdue University (1974).

14) Jaser M. Shabaki, Ph.D. thesis, Oregon State University (1976).

15) K.S. Krane, private communication.

16) K.S. Krane, Los Alamos Sci. Lab, Nuc. Inst. 4 Meth. 98, 205-210 (1972).

APPENDICES

APPENDIX A

Normalized values of Q_{22} and Q_{44} obtained from calibration using ^{22}Na source.

$Q_{22}(511 \text{ kev}) = 0.9287$

$Q_{44}(511 \text{ kev}) = 0.7795$

Table 8. Computed values of Ge(Li) detector finite solid angle correction factor Q_k for detector with D = 5 cm, L = 3.19 cm. (16)

Gamma ray energy (kev)	Q_2	Q_4
30	0.9146	0.7337
60	0.9167	0.7401
100	0.9225	0.7570
200	0.9337	0.7904
300	0.9373	0.8012
1000	0.9393	0.8074

APPENDIX B

Values of Q_{22} and Q_{44} for different energy cascades used in the experiment.

Table 9.

$Q_{22}(E\gamma_1, E\gamma_2)$	value	$Q_{44}(E\gamma_1, E\gamma_2)$	value
Q_{22}(322-139)	0.9268	Q_{44}(322-139)	0.7523
Q_{22}(280-180)	0.9208	Q_{44}(280-180)	0.7569
Q_{22}(280-107)	0.9127	Q_{44}(280-107)	0.7333
Q_{22}(420-139)	0.9174	Q_{44}(420-139)	0.7530
Q_{22}(252-280)	0.9248	Q_{44}(252-280)	0.7687
Q_{22}(252-322)	0.9257	Q_{44}(252-322)	0.7711
Q_{22}(252-387)	0.9259	Q_{44}(252-387)	0.7773
Q_{22}(252-460)	0.9261	Q_{44}(252-460)	0.7722